*Tellus (2004), 56B, 118–127*
*Printed in UK. All rights reserved*


**TELLUS**

# Retrieving the aerosol single-scattering albedo from the $NO_2$ photolysis rate coefficient

*By* H. RANDRIAMIARISOA[1*], P. CHAZETTE and G. MEGIE[2], [1]*Laboratoire des Sciences du Climat et de l'Environnement/IPSL, UMR CEA-CNRS 1572, Orme des Merisiers Bât 709, 91191 Gif-sur-Yvette, France;* [2]*Service d'Aéronomie/IPSL, Paris VI, Tour 15, 5 ème étage, 4, place Jussieu, 75252 Paris, France*

(Manuscript received 11 October 2002; in final form 24 September 2003)

ABSTRACT

A method for retrieving the aerosol single-scattering albedo $\omega_0$ in the ultraviolet region close to 400 nm within the atmospheric column is proposed based on a comparison between both $NO_2$ photolysis rate coefficients $J_{NO_2}$ measured by an optical actinometer under cloud-free conditions and $J_{NO_2}$ calculated using a radiative transfer model. This methodology is based on the sensitivity of $J_{NO_2}$ to $\omega_0$ variations as quantified using the radiative transfer model with particular emphasis on the aerosol extinction vertical profile. The method has been applied to assess $\omega_0$ within the framework of the Indian Ocean Experiment (INDOEX) over the Goa area located on the west coast of India. In the first place, the period under study was between March 2 and March 13, 1999 when ground-based lidar measurements were available. It has been further extended between February 25 and March 23, 1999 by making appropriate assumptions on the mean altitude of the aerosol layer. Taking into account the uncertainties related to each parameter introduced in the calculation (optical thickness, Ångström coefficient, asymmetry factor, surface albedo) and the model used, resulted in a total absolute accuracy on $\omega_0$ calculated to be 0.06 for observations close to local noon, and up to 0.07 for observations performed within 3 h before and after local noon. Results are less accurate for other times. For the 12 days under study, the values of $\omega_0$ calculated at noon range from 0.89 to 0.93. They vary weakly throughout the day with further differences being observed from one day to another. Such small variations in $\omega_0$ are in very good agreement with results obtained by other methods within the framework of the same campaign.

## 1. Introduction

Several studies have demonstrated the important impact of aerosols on the Earth's radiative budget and climate through their absorbing and scattering properties in the depth of the atmosphere (Hansen et al., 2000; IPCC 2001; Ramanathan et al., 2001). Depending on the magnitude of the aerosol absorption, they may either counterbalance or enhance the warming influence of globally increasing greenhouse gases. However, the radiative forcing by aerosols is more complex to evaluate than those of greenhouse gases and presents large uncertainties due to their high spatial and temporal variability caused by their shorter lifetimes in the atmosphere (IPCC 2001). By interacting with the solar radiation, aerosols also modify the actinic fluxes responsible for the photodissociation of gaseous molecules and may thus influence the magnitude of photochemical processes in the atmosphere. Indeed, observations and calculations made by Dickerson et al., (1997) indicate that scattering aerosols may increase ozone mixing ratios in the lower atmosphere, and that absorbing aerosols may reduce them. Accurate knowledge of the aerosol absorption property is thus fundamental and deserves extended studies.

The single-scattering albedo $\omega_0$ is a relevant parameter for characterizing the relative contribution of the aerosol particle absorption as compared to the scattering by the same particle. It is defined as the ratio between the scattering coefficient and the extinction (the sum of scattering and absorption) coefficient. It can take values between 0 (a purely absorbing particle) and 1 (a purely scattering particle) and can significantly evolve following both the activated aerosol sources and the ageing processes. For instance, a change in $\omega_0$ from 0.9 to 0.8 will change the sign of the direct effect of aerosols over particular ground surfaces (Hansen et al., 1997). During the INDOEX campaign, several independent methods found mean values of $\omega_0$ of between 0.83 and 0.93 either near the surface, or above the surface layer or within the atmospheric column (Ramanathan et al., 2001; Léon et al., 2002). Such changes in $\omega_0$ may influence the vertical balance of the low troposphere.

Several methods exist to estimate in situ values of $\omega_0$. They consist of measuring light transmitted and scattered by air samples as provided by complementary measurements from a

*Corresponding author.
e-mail: randria@lsce.saclay.cea.fr

nephelometer and a sunphotometer (Radke et al., 1991). Such a method requires very accurate calibration because the absorption, which is the difference between the extinction and the scattering, is often a difference between two large numbers. $\omega_0$ can also be derived from chemical analysis of the aerosol composition and its size distribution according to Mie theory. This last method requires assumptions on the particle shape and may be questionable with respect to the mixed composition of the absorbing elements as included in the aerosols (Ackerman and Toon, 1981; Li and Okada, 1999). Moosmüller et al., (1998) proposed direct measurements of light absorption using photoacoustic spectroscopy, for which the values were smaller compared with those from the filters technique. According to the authors, such results are possibly due to the difference of wavelengths at which the two techniques were performed. Well-calibrated sun photometers can also derive $\omega_0$ directly from sun/sky measurements (AERONET network) using the inversion methods of Dubovik et al., (2000). Most of the previous studies either give an average value or a time-localized value of $\omega_0$. Until now, there have been very few investigations to assess and study its daily variability.

In this paper we propose an iterative method to retrieve $\omega_0$ values of aerosol particles within the atmospheric column. The method, which requires cloud-free conditions, uses continuous measurements of the $NO_2$ photolysis rate coefficient $J_{NO_2}$ and a radiative transfer model. Indeed, several previous studies have looked at the sensitivity of $J_{NO_2}$ to the value of $\omega_0$ (Jacobson 1998; Castro et al., 2001) and a sensitivity study has also been performed in the present work. The $\omega_0$ retrieved by this method is defined at wavelengths close to 400 nm where the absorption of $NO_2$ is maximal, as will be shown later. The main objective of this work is to retrieve the diurnal as well as the day-to-day evolution of $\omega_0$. The data being used have been obtained during the international campaign INDOEX (Indian Ocean Experiment), which was dedicated to the study of polluted air masses transported from the Indian subcontinent throughout the Indian Ocean (Ramanathan et al., 2001). During the winter monsoon period (January to March of 1999), ground-based measurements of several aerosol properties were deployed at the coastal site of Goa (15.45°N, 73.08°E) and this paper is focused on the period between February 25 and March 23, 1999, which we consider as our intensive field phase, henceforth called IFP. During this winter monsoon, the prevailing winds were mostly northeasterly and the site of Goa is thus well located for observing characteristics of anthropogenic aerosols leaving the continent before they are mixed with the pristine air of the Indian Ocean (Léon et al., 2001). Preliminary values of $\omega_0$ derived from the present method have been previously presented in Léon et al., (2002) for the period between 11 and 23 of March 1999. However $\omega_0$ values were assessed without considering the spectral and the vertical dependences of aerosols. Indeed aerosols were assumed confined inside a layer between the surface and 2 km above the sea level in which the vertical extinction coefficient was supposed to be uniformly distributed. As will be shown, $\omega_0$ retrievals could be strongly sensitive to the aerosol vertical distribution, especially when the daily variability is investigated. In this paper, the period under study has been extended to cover the full period of the IFP between February 25 and March 23, including diurnal variations from 9 am to 3 pm, in order to assess the possible evolution of the aerosol characteristics throughout the day.

In a first section the methodology is presented including the description of the radiative transfer model used and the experimental context of INDOEX. The second section is focused on different sensitivity tests to study first the effects on the model calculated values of $J_{NO_2}$ of each of the aerosol parameters including their spectral dependence and secondly to emphasize the importance of the vertical repartition of the aerosol in terms of extinction. The objective is to assess the overall uncertainty on the retrieved value of $\omega_0$. In the third section, the results of diurnal and day to day evolutions of $\omega_0$ in the frame of the INDOEX campaign during the IFP are presented and compared with those obtained by other authors.

## 2. Methodology to retrieve the aerosol single-scattering albedo

### 2.1. Generality

The photolysis rate coefficient of nitrogen dioxide $NO_2$ is the probability for a $NO_2$ single molecule to be photodissociated by absorbing solar radiation.

$$J_{NO_2} = \int_{\Delta\lambda} \eta_{NO_2}(\lambda, T)\sigma_{NO_2}(\lambda, T)\Phi(\lambda)\mathrm{d}\lambda. \quad (1)$$

As given by the relation (1), it is a function of the $NO_2$ absorption cross section $\sigma_{NO_2}$ and its quantum yield $\eta_{NO_2}$, the actinic flux $\Phi$ and the temperature of the air parcel $T$. The spectral domain of $J_{NO_2}$ is defined by the product of both $\sigma_{NO_2}$ and $\eta_{NO_2}$. As shown in Fig. 1, the effective wavelength interval of $J_{NO_2}$ is mainly limited to the wavelengths from 300 to 420 nm, henceforth called $\Delta\lambda$ with maximum absorption close to 400 nm. $\Phi$ is sensitive to the presence of aerosols and can be itself considered as a function of the $\omega_0$, the vertical extinction coefficient $\alpha_{ext}(z)$ and the asymmetry factor $g$ of the aerosol.

$$J_{NO_2} = \int_{\Delta\lambda} \eta_{NO_2}(\lambda, T)\sigma_{NO_2}(\lambda, T)L(\lambda)\mathrm{d}\lambda.$$

### 2.2. Principle

The present method to retrieve $\omega_0$ for aerosol particles is based on a comparison between measured values of $J_{NO_2}$ in cloud-free conditions and $J_{NO_2}$ calculated using a radiative transfer model, for which $\omega_0$ is one of the input parameters. The high sensitivity of $J_{NO_2}$ as a function of $\omega_0$ as given by Fig. 2 constitutes the main reliability factor of this method. Following an iterative procedure, $\omega_0$ is tuned until agreement between measurements and calculations of $J_{NO_2}$ is reached in a predefined interval of

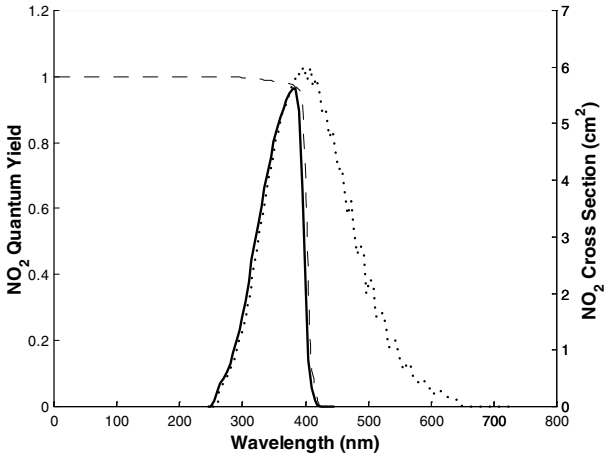


*Fig 1.* Absorption cross-section (dotted line) and quantum yield (dashed line) of $NO_2$ as a function of the wavelength. The product of these two quantities (solid line), which expresses the wavelength dependence of $J_{NO_2}$, is significant within the spectral range between 300 and 420 nm.

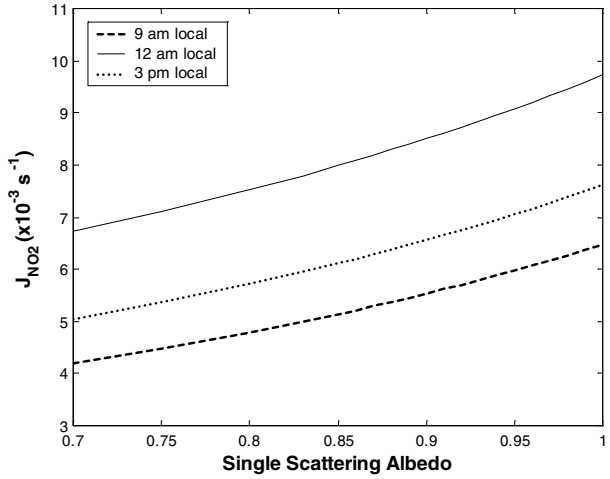


*Fig 2.* Sensitivity of $J_{N02}$ to $\omega_0$ variations at different Goa local time. The other parameters are fixed at their mean values observed during the IFP: $\xi = 0.1$, $g = 0.67$ (400 nm), $\tau_{440} = 0.72$ and Å $= 1.38$.

convergence. This interval is a function of the expected accuracy of the model measurement comparison of $J_{NO_2}$. In this retrieval process, the other input parameters remain fixed.

## 2.3. The radiative transfer model

The calculation of $J_{NO_2}$ is performed using actinic fluxes calculated with a radiative transfer model developed by S. Madronich and co-workers (Madronich and Flocke, 1998) called TUV (tropospheric ultraviolet and visible radiation model). This code is basically an extension to that used in many previous studies (Madronich, 1987; Madronich and Granier, 1992; Shetter et al., 1992; Lantz et al., 1996). Actinic fluxes of many gaseous species can be determined by TUV with an *n*-stream discrete ordinate radiative transfer method (Stamnes et al., 1988). The corresponding total $J_{NO_2}$ can be separate into its upward $J_{NO_2(up)}$ and its downward $J_{NO_2(down)}$ components. The input aerosol parameters are represented schematically in Fig. 3. They include the extinction vertical profile $\alpha_{ext}(z)$ and its spectral dependence defined by the Ångström coefficient Å, the asymmetry parameter $g$ and $\omega_0$.

Knowledge of the surface albedo $\xi$ is also required to perform the calculation. For this purpose, $\xi$ values throughout the day are first determined by iterative TUV calculations comparing the calculated and the measured ratios $J_{NO_2(up)}/J_{NO_2(down)}$ using a fixed value of $\omega_0$ ($= 0.9$). Then, the retrieved values of $\xi$ are used as input values in the radiative transfer model to assess new values of $\omega_0$. This iterative procedure is only reliable if $\xi$ is not too sensitive on $\omega_0$, which will be verified later.

## 2.4. Experimental measurements

During the INDOEX campaign, measurements of parameters required to assess $\omega_0$ as $J_{NO_2}$, $\alpha_{ext}(z)$, Å and $g$ were available at the Goa instrumental site which has been extensively described in a previous paper by Léon et al. (2001). It is therefore not detailed further here.

*2.4.1. Photolysis rate coefficient, $J_{NO_2}$.* Actinic fluxes have been measured by means of an optical actinometer (manufactured by Metcon, Glashütten, Germany). The absolute calibration to convert the actinic flux into $J_{NO_2}$ values is based on comparison with a chemical actinometer. The actinometer device is made up of two identical detectors with uniform response over $2\pi$ sr, which gives upward and downward actinic fluxes from which the values of $J_{NO_2(up)}$ and $J_{NO_2(down)}$ are determined. The measurement accuracy of the instrument is close to 5%. However, due to a failure of the downward part of the detector, $J_{NO_2(up)}$ and $J_{NO_2(down)}$ are only available simultaneously on 3 days during the IFP. Therefore, we mainly use $J_{NO_2(down)}$ values.

Figure 4 shows the daily evolution of $J_{NO_2}$ for March 4, 1999. The dotted curve represents $J_{NO_2}$ measured using the actinometer and the solid curve is the result of TUV simulations using the retrieved values of $\omega_0$. We note that with adequate input aerosol parameters, TUV can give values in good agreement with the measured value of $J_{NO_2}$. The maximum value of $J_{NO_2}$ during the day is observed close to local noon and ranges between $7 \times 10^{-3}$ $s^{-1}$ and $8 \times 10^{-3}$ $s^{-1}$ for the IFP period.

*2.4.2. Extinction coefficient $\alpha_{ext}(z)$ and Ångström coefficient Å.* The value of $\alpha_{ext}(z)$ is provided using micropulse lidar signals (Spinhirne, 1993) corrected with sun photometer data which provide the column-integrated aerosol optical thickness $\tau$ (Chazette, 2003). The relation between $\alpha_{ext}$ and $\tau$ is given by

$$\tau(z) = \int_0^\infty \alpha_{ext}(z)\mathrm{d}z. \quad (2)$$

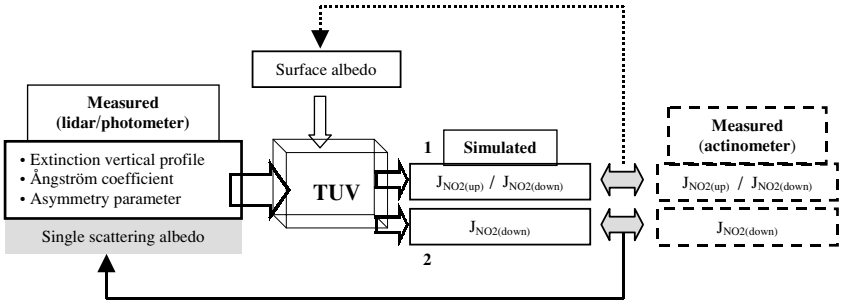


*Fig 3.* Schematic representation of the method used to retrieve the aerosol single-scattering albedo close to 400 nm (2) and the surface albedo (1) by iterative TUV calculations to best fit the measured values of $J_{NO_2(down)}$ and $J_{NO_2(up)}/J_{NO_2(down)}$ (with an actinometer) to their values estimated by a radiative transfer model (TUV).

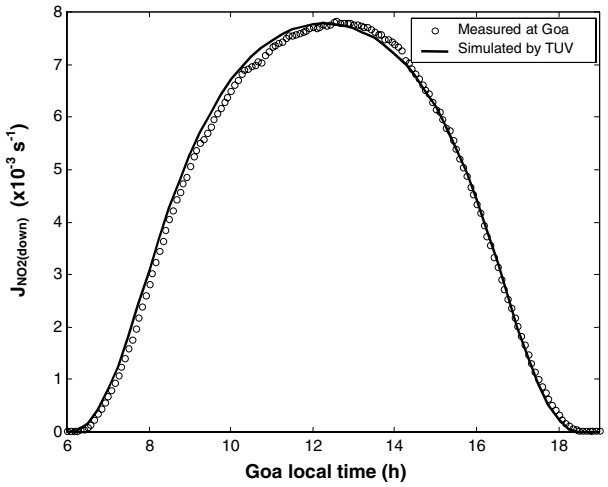


*Fig 4.* Measured and simulated downward component of the photolysis coefficient $J_{NO_2(down)}$ as a function of Goa local time on March 4, 1999.

Measurements of $\tau$ were performed at the following wavelengths: 440 nm ($\tau_{440}$), 670 nm ($\tau_{670}$) and 870 nm ($\tau_{870}$) and are available on the AERONET website. The Angström coefficient Å describing the spectral dependence of $\tau$ and $\alpha_{ext}$ can be derived in the visible domain from the values of $\tau_{440}$ and $\tau_{670}$ as given by the following Ångström relation:

$$\text{Å} = \frac{\ln\left(\frac{\tau_{670}}{\tau_{440}}\right)}{\ln\left(\frac{440}{670}\right)}. \quad (3)$$

The absolute accuracy on $\tau$ which essentially provides from the calibration error is 0.02 (Tanré et al., 1988). It results in an uncertainty in Å of about 7% (Hamonou et al., 1999). At local noon during the IFP, $\tau_{440}$ varied between 0.5 and 1.05 with an average value of 0.72 and Å varied between 1.17 and 1.5 with an average value of 1.38.

*2.4.3. Asymmetry factor g.* Using multispectral measurements of $\tau$ and multiangular sky radiance measurements, Dubovik et al. (2000) set up an inverse method which provides phase functions of the aerosol particles and from which $g$ values within the atmospheric column can be deduced. The relative accuracy of $g$ is estimated to be about 3%, according to the accuracy of the phase functions given by Dubovik et al. (2000). During the IFP, $g$ was fairly constant with values close to $0.67 \pm 0.02$ at 440 nm. At the surface, a three-wavelength nephelometer also gave $g$ values of between 0.55 and 0.65 at 440 nm (Léon et al., 2002).

### 2.5. *Assessment of the surface albedo*

The surface albedo $\xi$ was not measured at Goa and has been assessed following the iterative procedure (1) presented in Fig. 3 by best fitting the observed $J_{NO_2(up)}/J_{NO_2(down)}$ with those calculated by TUV with a fixed value of $\omega_0 = 0.9$. To assess the validity of this assumption, tests have been conducted by calculating $\xi$ values when $\omega_0$ varied in a range between 0.7 and 1. This interval corresponds to reasonable values of $\omega_0$ for anthropogenic aerosols (Ramanathan et al., 2001). As shown in Fig. 5, $\xi$ appears to vary weakly with $\omega_0$ changes for each considered time of day.

$\xi$ is a function of the solar zenith and azimuth angles, and its diurnal variability has to be taken into account. $J_{NO_2(up)}$ and

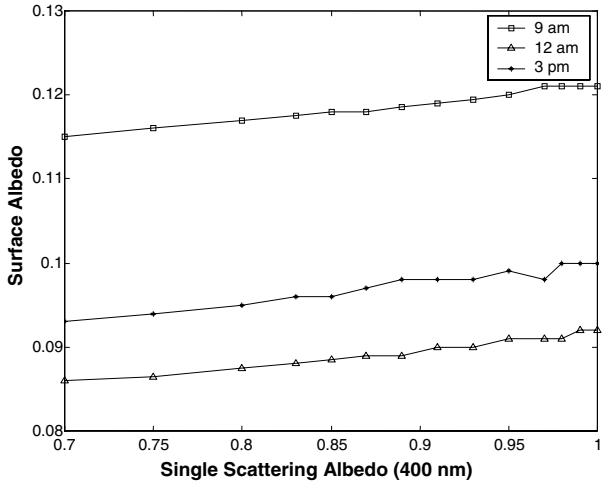


*Fig 5.* Surface albedo for different values of $\omega_0$ as retrieved at different Goa local time by iterative TUV calculations to best fit the measured and the simulated values of $J_{NO_2(up)}/J_{NO_2(down)}$. The other parameters are fixed at their mean values observed during the IFP: $g = 0.67$ (440 nm), $\tau_{440} = 0.72$, and Å $= 1.38$.

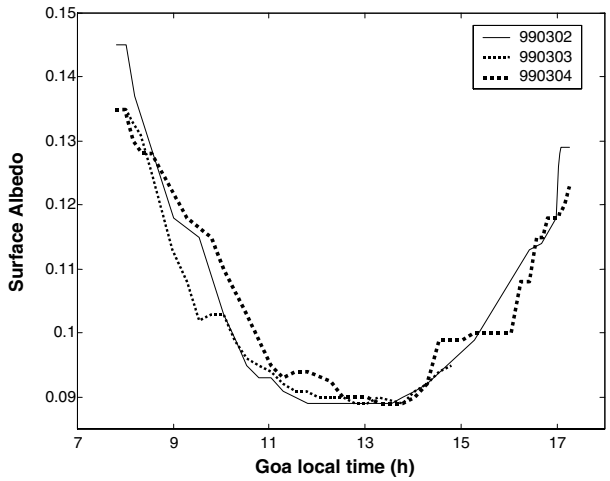


*Fig 6.* Daily variations of the surface albedo as retrieved by iterative TUV calculations to best fit the observed ratio $J_{NO_2(up)}/J_{NO_2(down)}$ for the spectral region between 300 and 400 nm at the site of Goa. The values presented were obtained during three days when measured values of $J_{NO_2(up)}$ and $J_{NO_2(down)}$ were available simultaneously.

$J_{NO_2(down)}$ were simultaneously available for only 3 days during the campaign. However it is sufficient to assess the temporal evolution of $\xi$, as the surface characteristics of the site, which mainly correspond to a semi-arid surface did not change during the IFP. The simulations were performed with a mean representative aerosol loading observed during the IFP over Goa corresponding to $\tau_{440} = 0.72, \text{Å} = 1.38$ and $g = 0.67$ at 440 nm.

Figure 6 shows that $\xi$ varies between 0.09 and 0.14 with a minimum value close to local noon for the spectral region between 300 and 400 nm. Hereafter we shall use the hourly mean value of $\xi$ as calculated over these 3 days.

## 3. Sensitivity studies

### 3.1. Spectral dependence of the aerosol parameters

The behaviour of $\omega_0$, $g$ and Å as a function of the wavelength $\lambda$ were simulated by means of Mie theory using both aerosol size distributions and refractive indices as measured from the AERONET network. The results are shown in Fig. 7 for the spectral interval $\Delta\lambda$ of interest between 300 and 400 nm.

*3.1.1. Asymmetry factor.* Results indicate a linear dependence of $g(\lambda)$ within $\Delta\lambda$ as already demonstrated by Ross and Hobbs (1998). This linearity was taken into consideration to calculate $J_{NO_2}$ in the TUV model by introducing values of $g$ at two wavelengths retrieved from sun photometer measurements (AERONET network).

*3.1.2. Ångström coefficient.* Within $\Delta\lambda$, Å $(\lambda)$ is quasi-linear with a variation of 8% compared with a mean value of 1.23 at 400 nm. However, measurements of Å are only available in the wavelength range between 440 and 670 nm, which can correspond in Fig. 7 to a maximum value of $\text{Å} = 1.33$. The difference between 1.33 and 1.23 is close to 7%. Considering this 7% and the previous 8% variation within $\Delta\lambda$, the uppermost uncertainty from the spectral dependence of Å can thus be considered to be close to 11%.

*3.1.3. Single-scattering albedo.* $\omega_0(\lambda)$ is fairly constant within $\Delta\lambda$ with less than 0.6% variation.

Therefore Å$(\lambda)$ and $\omega_0(\lambda)$ will be considered constant in the TUV model calculations. Nevertheless, the corresponding reduction of accuracy on the retrieved values of $\omega_0$ induced by such spectral variations will be assessed and considered in the total error budget.

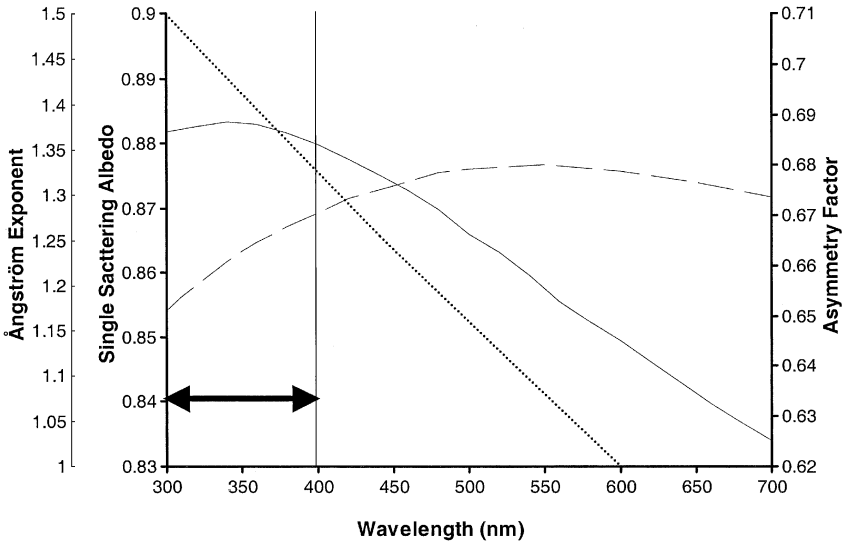


*Fig 7.* Spectral dependences of the Ångström coefficient (dashed line), the asymmetry factor (dotted line), and the single-scattering albedo (solid line) in the case of the mean aerosol characteristics retrieved over Goa during INDOEX. Interval to be considered is between 300 nm and 400 nm (solid arrow).

### 3.2. *Influence of scalar parameters*

Studies were conducted to observe the behaviour of $J_{NO_2}$ derived from TUV model calculations when other parameters are varying. In these sensitivity tests, the uncertainties from the measurement, and the assessment or the spectral dependence of each input parameter are taken into account in order to evaluate their impact on the calculated $J_{NO_2}$. The variability of the solar zenith angle is always considered by performing simulations at different representative local time: 9 am, 12 am and 3 pm.

*3.2.1. Surface albedo.* As shown in Fig. 8, $J_{NO_2}$ is an increasing function of $\xi$ with an increased sensibility close to local noon. Knowing the uncertainties on $\xi$ from the previous assessment, its expected relative impact on $J_{NO_2}$ is close to 2%, 1% and 2%, respectively, at 9 am, 12 am and 3 pm.

*3.2.2. Optical thickness.* $J_{NO_2}$ is very sensitive to $\tau_{440}$ as shown in Fig. 9 as an increase of $\tau_{440}$ induces an important decrease of $J_{NO_2}$. For $\tau_{440} = 0.72$, an absolute uncertainty of 0.02 corresponds to uncertainties close to 1% on $J_{NO_2}$.

*3.2.3. Ångström coefficient.* A decrease in $J_{NO_2}$ when Å is increasing is observed in Fig. 10 showing a non-negligible sensitivity. Knowing the uncertainties on Å (from its assessment and from Å(λ)), the impact of Å on $J_{NO_2}$ may lead to relative uncertainties of 2%, 1% and 1%, respectively, at 9 am, 12 am and 3 pm.

*3.2.4. Asymmetry factor.* Figure 11 shows $J_{NO_2}$ as a function of $g$. $J_{NO_2}$ appears to be weakly sensitive to variations in $g$ with a relative impact smaller than 0.75%. The spectral dependence of $g$ has been considered in the simulations.

Table 1 summarizes the different uncertainties on $J_{NO_2}$ at different times of day.

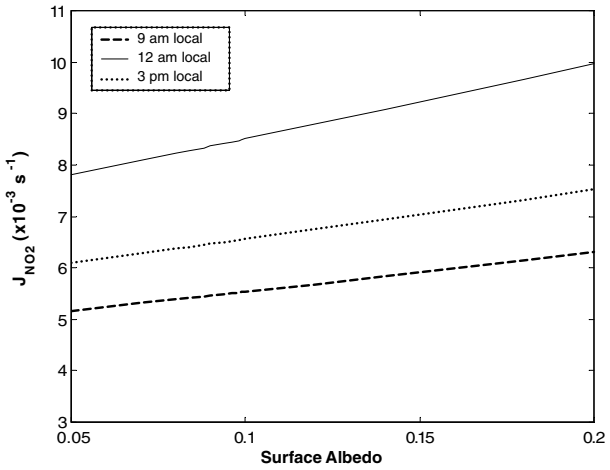


*Fig 8.* Sensitivity of $J_{N02}$ to variations in the surface albedo at different Goa local time. The other parameters are fixed at their mean values observed during the IFP: $\omega_0 = 0.9$, $g = 0.67$ (440 nm), $\tau_{440} = 0.72$ and Å $= 1.38$.

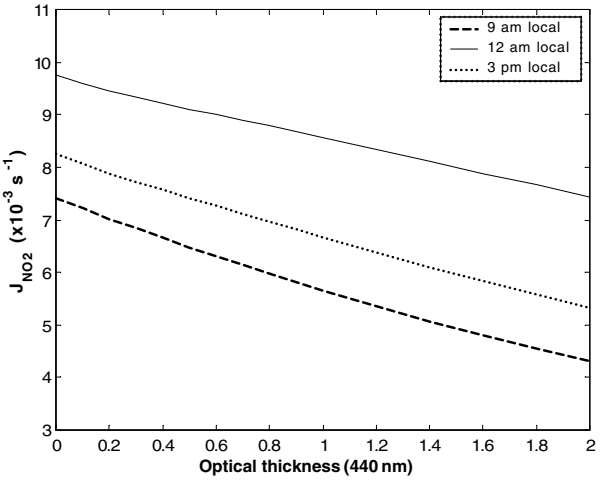


*Fig 9.* Sensitivity of $J_{N02(down)}$ to variations in the optical thickness at different Goa local time. The other parameters are fixed to their mean values observed during the IFP: $\xi = 0.1$, $\omega_0 = 0.9$, $g = 0.67$ (440 nm) and Å $= 1.38$.

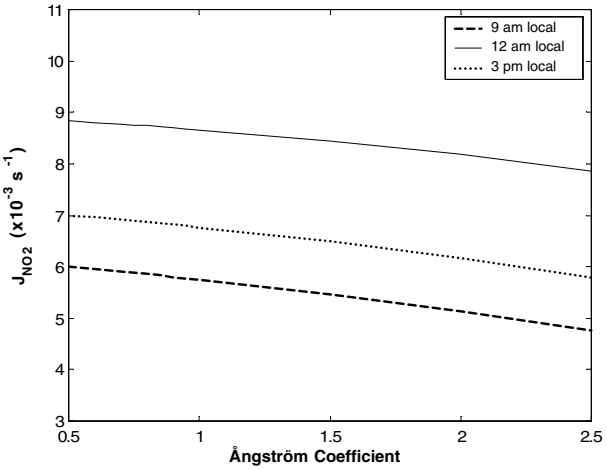


*Fig 10.* Sensitivity of $J_{N02}$ to variations in the Ångström coefficient at different Goa local time. The other parameters are fixed to their mean values observed during the IFP: $\xi = 0.1$, $\omega_0 = 0.9$, $g = 0.67$ and $\tau_{440} = 0.72$.

### 3.3. *Influence of the aerosol vertical profile*

Knowledge of the vertical profile of the aerosol extinction coefficient is required for a correct assessment of the actinic flux, and thus of $\omega_0$. As an example, we will consider three different layers between 0 and 1 km, 0 and 1.5 km, and 0 and 2 km, respectively. In each layer, $\alpha_{ext}(z)$ is assumed to be constant, i.e. all the aerosols are uniformly distributed from the surface to the top of the layer, in relation with $\tau$ measured by the sun photometer knowing the relation between $\tau$ and $\alpha_{ext}$. For these different assumptions on the vertical distribution of the aerosols, Fig. 12 gives the evolution of $\omega_0$ at local noon from February 25 to March 23. A significant difference on the retrieval of $\omega_0$

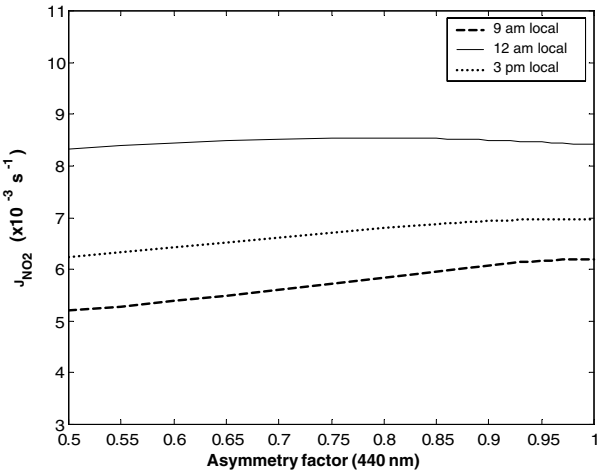


*Fig 11.* Sensitivity of $J_{NO_2}$ to variations in the asymmetry factor at different Goa local time. The other parameters are fixed to their mean values observed during the IFP: $\xi = 0.1$, $\omega_0 = 0.9$, $\tau_{440} = 0.72$ and Å $= 1.38$.

exists depending on the altitude of the top layer. Indeed, a difference of 1 km in the layer top height may lead to a difference of up to 0.08 on the retrieved value of $\omega_0$. Realistic profiles of the aerosol vertical distribution are thus required for each case to more precisely assess $\omega_0$.

### *3.4. Total uncertainty on the retrieval of $\omega_0$*

The total uncertainty on the retrieval of $\omega_0$ is provided by the uncertainties summarized in Table 1 for $J_{NO_2}$ calculated, $J_{NO_2}$ measured and the model used. These different sources of error playing a role in the assessment of $\omega_0$ can be considered independent. The absolute uncertainty on the retrieved value of $\omega_0$ is thus estimated to be close to 0.07, 0.06 and 0.07, respectively, at 9 am, 12 am and 3 pm. Outside this time period, the signal-to-noise ratio in the actinometer measurements becomes too weak to derive $\omega_0$ with reasonable accuracy.

## 4. Results and discussion

### *4.1. Daily variability*

Continuous measurements of $J_{NO_2}$ (recorded every 5–10 min) enable one to derive the evolution of $\omega_0$ between 9 am and 3 pm. As the importance of the knowledge of the vertical distribution of $\alpha_{ext}(z)$ was underlined above, profiles from lidar measurements were used in the retrieval of $\omega_0$. Figure 13 shows the results for these retrievals for the period between March 2 and 13, when lidar measurements were available at Goa (Chazette, 2003). Even if the behaviour of $\omega_0$ appears to be different from one day to

*Table 1.* Absolute accuracy of the retrieved $\omega_0$ by the present method derived from the different uncertainties as related to measurements and to assessment of each used parameter and to model used

| | Uncertainties from measurement/assessment | Uncertainties from spectral dependence | Goa local time | !mpact on $J_{NO_2}$ calculated | |
|---|---|---|---|---|---|
| $J_{NO_2}$ | 5% (Metcon instrumentation) | | | 5% | |
| $J_{NO_2}$ | 5% (Model using: Madronich and Flocke, 1998) | | | 5% | |
| Aero. extinct. profile | 5% (Chazette, 2003) | | | 3% | |
| Ångström exp. | 7% (Hamonou et al., 1999) | 11% (this paper) | 9 am | 2.30% | |
| | | | 12 am | 1.19% | |
| | | | 3 pm | 2.23% | |
| Surface albedo | 3% (this paper) | | 9 am | 2% | |
| | 2% (this paper) | | 12 am | 1% | |
| | 3% (this paper) | | 3 pm | 2% | |
| Column. opt. thick. | 0.02 (Dubovik et al., 2000) | | 9 am | 1.30% | |
| | | | 12 am | 0.60% | |
| | | | 3 pm | 1.00% | |
| Asymmetry param. | 3% (this paper) | | 9 am | 0.74% | |
| | | | 12 am | 0.08% | |
| | | | 3 pm | 0.60% | |
| | | | | Total impact on $J_{NO_2}$ calculated | Accuracy expected on the retrieved sing. scat. alb. |
| | | | 9 am | 8.39% | ±0.07 |
| | | | 12 am | 7.86% | ±0.06 |
| | | | 3 pm | 8.30% | ±0.07 |

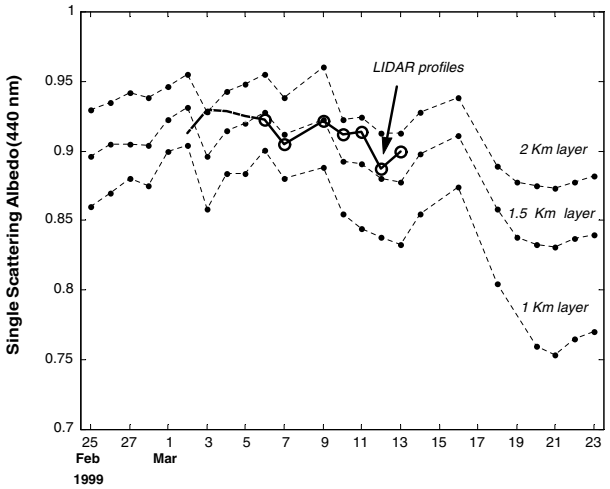


*Fig 12.* Influence at Goa local noon of the aerosol vertical distribution on $\omega_0$ retrievals (∼400 nm) by assuming different uniform aerosol layers of 1, 1.5 and 2 km top height (dotted curves), and experimental vertical profiles of aerosol extinction coefficient as obtained from lidar measurements (solid curve).

one another, its variation throughout the day remains relatively small with an average value close to 0.91 (∼400 nm). Chazette (2003) showed that the backscatter to extinction ratio values (*BER*) as deduced from lidar measurements remains constant throughout the day during the whole IFP. As $BER = \omega_0 P_\pi$, where $P_\pi$ is the backscatter phase function, this confirms the present results that the value of $\omega_0$ is relatively constant and indicates that the characteristics of the atmospheric aerosols are only weakly varying.

### 4.2. *Day-to-day variability*

Reconsidering the particular case of observations made at local noon, the retrieved values of $\omega_0$ using lidar profiles from March 2 to 13 ranges between 0.88 and 0.93 close to 400 nm (Fig. 11). Such variability remains within the uncertainty range of ±0.06 previously assessed. This variability could thus be non-significant in agreement with the results presented in Chazette (2003). Nevertheless according to Fig. 12, retrieved values of $\omega_0$ using the lidar data are shown to be close to those provided from uniform aerosol layers with top height at 1.5 km and at 2 km of altitude. We have thus assumed for the whole IFP period that the top height of the equivalent monsoon layer at Goa is situated between 1.5 and 2 km above the surface. Such an assumption may be helpful for analysis of a larger period of measurements even if lidar data were not available. As a result, Fig. 12 shows that the value of $\omega_0$ retrieved at local noon significantly decreases after March 16 from ∼0.91 to ∼0.83. The same behaviour is noted when performing calculation of $\omega_0$ at 9 am and 3 pm during the same IFP. This might relate to a change in the characteristics of the aerosol particle, related to a larger absorption as discussed hereafter.

### 4.3. *Discussion*

Ramanathan et al. (2001) summarized values of $\omega_0$ over the Indian Ocean derived by various methods. For instance, they range between 0.85 and 0.9 for the near surface using filters and cascade impactors data (Chowdhury et al., 2001; Lelieveld et al., 2001) or from nephelometer data coupled with PSAP measurements, and between 0.8 and 0.9 above the surface layer from aircraft coupled with lidar data. For the present study, $\omega_0$ is

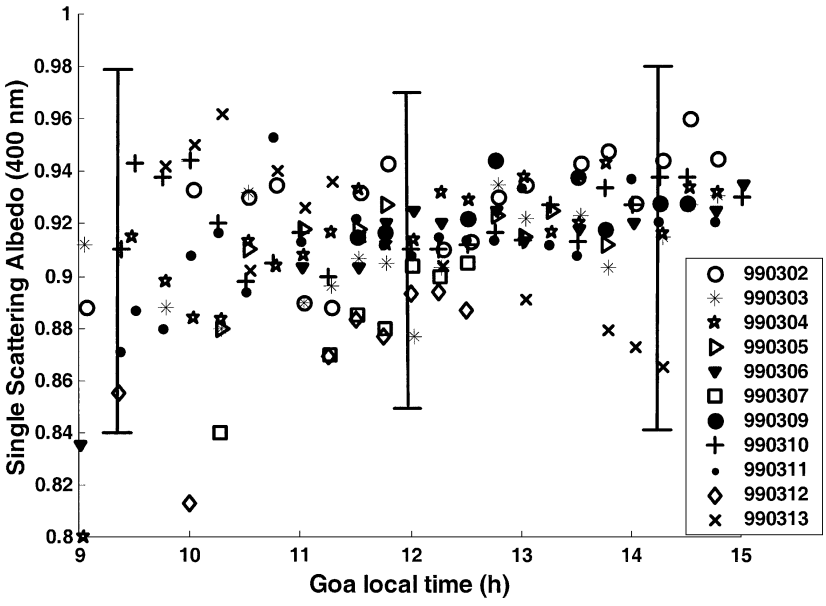


*Fig 13.* Diurnal variations of $\omega_0$ (∼400 nm) during INDOEX for the period where lidar measurements were available. The vertical bars represent the absolute accuracy at different times.

representative of the whole atmospheric column. As an example in Kashidoo, at 700 km to the south of the Indian subcontinent, column average values of $\omega_0$ between 0.86 and 0.9 are derived using a radiative transfer model and photometer/radiometer measurements (Satheesh et al., 1999). Although these results are in agreement with those presented in the present paper, the difference in the geographical location of the two sites should lead to different characteristics of the aerosol. Kashidoo is indeed characterized by its remote location away from major human sources, while Goa is located close to pollution sources from the continent. As already noted by Ramanathan et al. (2001), the narrow range observed for the mean $\omega_0$ values in the whole region (0.85–0.9) is surprising in view of the different sources and processes which should influence the formation and the evolution of the continental aerosol. This might be due to the aerosol sources being widespread and the mixing of the aerosol by the persistence of the monsoon flow. All the retrieved $\omega_0$ values correspond to highly absorbing aerosol particles. The aerosol absorption observed during INDOEX results mainly from carbon originating from biomass burning and fossil fuel combustion, and with a smaller contribution from mineral dust (Satheesh et al., 1999; Schwartz and Buseck 2000). Two hypotheses might be formulated to explain the decrease observed after March 16 in $\omega_0$ (Fig. 12): either an increase activity in biomass burning as documented by Léon et al. (2002) or the arrival of dust particles from the African continent and the Arabian Peninsula. For the former assumption, there might be an important production of small particles, which could lead due to the coating phenomenon to an increase in the absorption (Redeman et al., 2001). For the latter assumption, dust particles are more absorbing and the mixture with the anthropogenic aerosols may result in lower values of $\omega_0$ (Takemura et al., 2002).

## 5. Conclusion

An iterative method based on a comparison between $J_{NO_2}$ measured by an optical actinometer and $J_{NO_2}$ calculated by a radiative transfer model TUV (Madronich and Flocke, 1998) has been used to retrieve the aerosol particles single-scattering albedo $\omega_0$ within the atmospheric column. The method has been applied to evaluate $\omega_0$ close to 400 nm during the winter monsoon of 1999 at Goa in the frame of the INDOEX campaign. Vertical profiles of the extinction coefficient have been shown to be required for such a retrieval and were obtained from lidar measurements. The total absolute uncertainty on $\omega_0$ has been estimated to be 0.06 close to local noon and 0.07 close to 9 am and 3 pm. Throughout the day there is practically no variation of $\omega_0$ values with an average value of 0.91. As for the day-to-day evolution at local noon, $\omega_0$ also does not vary during the period from March 2 to 13, for which lidar data were available to retrieve the altitude dependence of the aerosol extinction. When extrapolating these results over a longer period of time assuming an average aerosol layer with top height between 1.5 and 2 km above the surface, a significant decrease in $\omega_0$ values from 0.9 to 0.83 is observed after March 16. Such a behaviour may be due to the presence of more absorbing aerosol particles linked to more intensive biomass burning or to mixing with dust particles. The $\omega_0$ values derived from the present work are in good agreement with those assessed by other methods. All the retrieved $\omega_0$ values in this region indicate a remarkably large absorption component of the aerosol particles, which should certainly be taken into account for a more quantitative determination of the anthropogenic contribution of the aerosol to the radiative forcing.

## 6. Acknowledgements

This work has been funded by the CNRS/INSU Programme National de Chimie Atmosphérique, the Commissariat à l'Energie Atomique and the PSA Peugeot Citröen.

## References

Ackerman, P. T. and Toon, O. B. 1981. Absorption of visible radiation in the atmosphere containing mixtures of absorbing and non-absorbing particles. *Appl. Opt.* **20**, 3661–3667.

Ångström, A. 1964. The parameters of atmospherics turbidity. *Tellus* **16**, 64–75.

Castro, T., Madronich, S., Rivale, S., Muhlia, A. and Mar, B. 2001. The influence of aerosols on photochemical smog in Mexico city. *Atmos. Environ.* **35**, 1765–1772.

Chazette, P. 2003. Optical properties of the aerosol column observed during INDOEX at the coastal site of Goa. *J. Geophys. Res.* **108** (D6), 4187, doi:10.209 /2002JD002074.

Chowdhury, Z., Hughes, L. S., Salmon, L. G. and Cass, G. R. 2001. Atmospheric particle size and composition measurements to support light extinction calculations over the Indian Ocean. *J. Geophys. Res.* **106**, 28 597–28 606.

Dickerson, R. R., Kondragunta, S., Stenchikov, G., Civerolo, K. L., Doddgridge, B. G. and Holben, B. N. 1997. The impact of aerosols on solar ultraviolet radiation and photochemical smog. *Science* **278**, 827–830.

Dubovik, O., Smirnov, A., Holben, B. N., King, M. D., Kaufman, Y. J., Eck, T. F. and Slutsker, I. 2000. Accuracy assessments of aerosol optical properties retrieved from aerobotic Network (AERONET) Sun and sky radiance measurements. *J. Geophys. Res.* **105**, 9791–9806.

Hamonou, E., Chazette, P., Balis, D., Dulac, F., Schneider, X., Galani, E., Ancellet, G. and Papayannis, A. 1999. Characterization of the vertical structure of Saharan dust export to the Mediterranean basin. *J. Geophys. Res.* **104**, 22 257–22 270.

Hansen, J. E., Sato, M. and Ruedy, R. 1997. Radiative forcing and climate response. *J. Geophys. Res.* **102**, 6831–6864.

Hansen, J., Sato, M., Ruedy, R., Lacis, A. and Oinas, V. 2000. Global warming in the twenty-first century: an alternative scenario. *Proc. Natl. Acad. Sci., USA* **97**, 9875–9880.

IPCC 2001. *Climate change 2000:* The scientific basis contribution of working group I to the Third Assessment Report of the Intergovernmental Panel on Climate Change. Cambridge University Press, Cambridge, 1–881.

Jacobson, M. 1998. Studying the effects of aerosols on vertical photolysis rate coefficient and temperature profiles over an urban airshed. *J. Geophys. Res.* **103**, 10 593–10 604.

Lantz, K. O., Shetter, R. E., Cantrell, C. A., Flocke, S. J., Calvert, J. G. and Madronich, S. 1996. Theoretical, actinometric, and radiometric determinations of the photolysis rate coefficient of $NO_2$ during MLOPEX II. *J. Geophys. Res.* **101**, 14 613–14 629.

Lelieveld, J., Crutzen, P. J., Ramanathan, V., Andreae, M. O., Brenninkmeijer, C., Campos, T., Cass, G. R., Dickerson, R. R., Fischer, H. and De Gouw, J. A. 2001. The Indian Ocean Experiment: widespread air pollution from South and Southeast Asia. *Science* **5506**, 1031–1035.

Léon, J.-F., Chazette, P., Dulac, F., Pelon, J., Flamant, C., Bonazzola, M., Foret, G., Alfaro, S. C., Cachier, H. and Cautenet, S. 2001. Large scale advection of continental aerosols during INDOEX. *J. Geophys. Res.* **106**, 28 427–28 440.

Léon, J.-F., Chazette, P., Pelon, J., Dulac, F. and Randriamiarisoa, H. 2002. Aerosol direct radiative impact over the INDOEX area based on passive and active remote sensing. *J. Geophys. Res.* **107**(D19), 8006, doi:10.1029/2000JD000116.

Li, F. and Okada, K. 1999. Diffusion and modification of marine aerosol particles over the coastal areas in China: a case study using a single particle analysis. *J. Atmos. Sci.* **56**, 241–248.

Madronich, S. 1987. Photodissociation in the atmosphere 1. Actinic flux and effects of ground reflections and clouds. *J. Geophys. Res.* **92**, 9740–9752.

Madronich, S. and Flocke, S. 1998. The role of solar radiation in atmospheric chemistry. In: *Handbook Environmantal Chemistry* (ed. P. Boule). Springer-Verlag, Berlin, 1–26.

Madronich, S. and Granier, C. 1992. Impact of recent total ozone changes on tropospheric ozone photodissociation, hydroxyl radicals, and methane trends. *Geophys. Res. Lett.* **19**, 465–467.

Moosmüller, H., Arnott, W. P., Rogers, C. F., Chow, J. C., Frazier, C. A., Sherman, L. E. and Dietrich, D. L. 1998. Photo-acoustic and filter measurements related to aerosol light absorption during the Northern Front Range Quality Study (Colorado 1996/1997). *J. Geophys. Res. Atmos.* **103**, 28 749–28 157.

Radke, L. F., Hegg, D. A., Hobbs, P. V., Nance, J. D., Lyons, J. H., Laursen, K. K., Reagan, P. J. and Ward, D. E. 1991. Particulate and trace gas emission from large biomass fires in North America. *Global Biomass Burning*. MIT Press, Cambridge, MA, 209–224.

Ramanathan, V., Crutzen, P. J., Lelieveld, J., Althausen, D., Anderson, J., Andreae, M. O., Cantrell, W., Cass, G. and Chung, C. E. 2001. The Indian Ocean Experiment: an integrated assessment of the climate forcing and effects of the great Indo-Asian haze. *J. Geophys. Res.* **106**, 28 371–28 398.

Redeman, J., Russel P. B. and Hamill, P. 2001. Dependence of aerosol light absorption and single scattering albedo on ambient relative humidity for sulfate aerosols with black carbon cores. *J. Geophys. Res.* **106**, 27 485–27 495.

Ross, J. L. and Hobbs, P. V. 1998. Radiative characteristics of regional hazes dominated by smoke from biomass burning in Brazil: closure tests and direct radiative forcing. *J. Geophys. Res.* **103**, 31 925–31 991.

Satheesh, S. K., Ramanathan, V., Li-Jones, X., Lobert, J. M., Podgorny, I. A., Prospero, J. M., Holben, B. N. and Loeb, N. G. 1999. A model for the natural anthropogenic aerosols over the tropical Indian Ocean derived from the Indian Ocean Experiment data. *J. Geophys. Res.* **104**, 27 421–27 440.

Schwartz, S. E. and Buseck, P. R. 2000. Absorbing phenomena. *Science* **288**, 989–990.

Shetter, R. E., McDaniel, A. H., Cantrell, C. A., Madronich, S. and Calvert, J. G. 1992. Actinometer and Eppley radiometer measurements of the $NO_2$ photolysis rate coefficient during MLOPEX. *J. Geophys. Res.* **97**, 10 349–10 359.

Spinhirne, J. D. 1993. Micropulse lidar. IEEE Trans. *Geo. Rem. Sens.* **31**, 48–55.

Stamnes, K., Tsay, S., Wiscombe, W. J. and Jayaweera, K. 1988. Numerically stable algorithm for discrete-ordinate-method radiative transfer in multiple scattering and emitting layered media. *Appl. Opt.* **27**, 2502–2509.

Takemura, T., Nakajima, T., Dubovik, O., Holben, B. N. and Kinne, S. 2002. Single scattering albedo and radiative forcing of various aerosol species with a global three-dimensional model. *J. Climate* **15**, 333–352.

Tanré, D., Devaux, C., Herman, M. and Santer, R. 1988. Radiative properties of desert aerosols by optical ground-based measurements at solar wavelengths. *J. Geophys. Res.* **93**, 14 223–14 231.